

**GALLOBEUDANTITE, $\text{PbGa}_3[(\text{AsO}_4)_2(\text{SO}_4)]_2(\text{OH})_6$,
A NEW MINERAL SPECIES FROM TSUMEB, NAMIBIA,
AND ASSOCIATED NEW GALLIUM ANALOGUES
OF THE ALUNITE – JAROSITE FAMILY**

JOHN L. JAMBOR

Department of Earth Sciences, University of Waterloo, Waterloo, Ontario N2L 3G1

DeALTON R. OWENS

CANMET, 555 Booth Street, Ottawa, Ontario K1A 0G1

JOEL D. GRICE

Research Division, Canadian Museum of Nature, P.O. Box 3443, Station D, Ottawa, Ontario K1P 6P4

MARK N. FEINGLOS

Duke University Medical Center, Box 3921, Durham, North Carolina 27710, U.S.A.

ABSTRACT

Gallobeudantite, ideally $\text{PbGa}_3[(\text{AsO}_4)_2(\text{SO}_4)]_2(\text{OH})_6$, is the newly defined Ga analogue of beudantite. It occurs as zoned rhombohedra, up to 200 μm along an edge, in vugs in a single specimen of massive Cu-bearing sulfides from Tsumeb, Namibia. Gallobeudantite is variably pale yellow, greenish, or cream-colored, with a white to pale yellow streak, vitreous luster, even to conchoidal fracture, hardness of 4, and $D(\text{calc.})$ 4.61 g/cm^3 for $Z = 3$. The mineral is nonpleochroic, uniaxial negative, ω 1.763(5), ϵ 1.750(5). A single-crystal X-ray refinement of the structure ($R = 0.078$) showed the mineral to be rhombohedral, space group $R\bar{3}m$, a 7.225(4), c 17.03(2) Å, and isostructural with corkite. The strongest lines of the X-ray powder-diffraction pattern [d in Å(hkl)] are: 5.85(90)(101), 3.59(40)(110), 3.038(100)(113) and 2.271(40)(107). Within the crystals, in addition to gallobeudantite, are zones containing Ga-rich beudantite and hidalgoite, and the unnamed Ga analogues of segnitite, corkite, kintoreite, and arsenocrandallite. The last contains up to 12.7 wt.% GeO_2 , which is about 75% of the Ge substitution possible if the formula is assumed to be $\text{Ca}(\text{Ga,Al,Fe})_2\text{Ge}^{4+}(\text{AsO}_4)_2(\text{OH})_6$. The new name gallobeudantite alludes to the predominance of Ga in the position occupied by Fe^{3+} in beudantite-type minerals.

Keywords: gallobeudantite, new mineral species, description, crystal structure, alunite – jarosite family, gallium analogue, nomenclature, Tsumeb, Namibia.

SOMMAIRE

La gallobeudantite, de composition idéale $\text{PbGa}_3[(\text{AsO}_4)_2(\text{SO}_4)]_2(\text{OH})_6$, est l'équivalent gallifère nouvellement décrit de la beudantite. Elle se présente en rhomboèdres zonés, jusqu'à 200 μm de côté, dans les cavités d'un seul échantillon de sulfures massifs de cuivre provenant de Tsumeb, en Namibie. La gallobeudantite a une couleur variable, jaune pâle, verdâtre, ou crème; elle possède une rayure blanche à jaune pâle, un éclat vitreux, une cassure égale à conchoïdale, une dureté de 4, et une densité calculée de 4.61 g/cm^3 pour $Z = 3$. C'est un minéral non pleochroïque, uniaxe négatif, ω 1.763(5), ϵ 1.750(5). Un affinement de la structure ($R = 0.078$) montre qu'il s'agit d'un minéral rhomboédrique, groupe spatial $R\bar{3}m$, a 7.225(4), c 17.03(2) Å, ayant la même structure que la corkite. Les raies les plus intenses du spectre de diffraction (méthode des poudres) [d en Å(hkl)] sont: 5.85(90)(101), 3.59(40)(110), 3.038(100)(113) et 2.271(40)(107). A l'intérieur des cristaux, en plus de la gallobeudantite, se trouvent des zones contenant beudantite riche en Ga et hidalgoite, et les analogues à Ga de segnitite, corkite, kintoreite, et arsenocrandallite, toujours sans noms. Cette dernière contient jusqu'à 12.7% GeO_2 (poids), ce qui est environ 75% du remplacement possible par le Ga si on suppose la formule $\text{Ca}(\text{Ga,Al,Fe})_2\text{Ge}^{4+}(\text{AsO}_4)_2(\text{OH})_6$. Le nom de l'espèce nouvelle, gallobeudantite, fait allusion à la prédominance du Ga dans la position du Fe^{3+} dans les minéraux de type beudantite.

Keywords: gallobeudantite, nouvelle espèce minérale, description, structure cristalline, famille de l'alunite et de la jarosite, analogue à gallium, nomenclature, Tsumeb, Namibie.

INTRODUCTION

Gallite, CuGaS_2 , and söhngelite, $\text{Ga}(\text{OH})_3$, originally described from occurrences at Tsumeb, Namibia, are the only previously well-defined minerals containing Ga as an essential constituent. The Ga analogue of jarosite $\text{KGa}_3(\text{SO}_4)_2(\text{OH})_6$ was synthesized by Dutrizac (1984), who demonstrated that Ga substitutes for Fe in jarosite-type structures, and that the resulting solid-solutions are nearly ideal chemically. We report here on the natural occurrence of extensive Ga substitutions in minerals of the jarosite – alunite family as found in a single specimen from Tsumeb, Namibia. Included in the description is the new species name gallobeudantite, which has been approved by the Commission on New Minerals and Mineral Names, IMA.

Most Ga is commercially produced as a by-product from the treatment of bauxite ores, but the Apex mine in Utah was unique in that it operated briefly in the late 1980s solely for the purpose of producing Ga and Ge. These elements at Apex are contained in limonitic ores derived by the oxidation of Cu–Pb–Zn–Ag sulfide veins in dolomite (Bernstein 1986, Hopkins 1985). Jarosite from the Apex deposit was reported to contain up to 0.70 wt.% Ga (Dutrizac *et al.* 1986). The new name *gallobeudantite* alludes to the predominance of Ga in the position occupied by Fe^{3+} in jarosite-type minerals. The original specimen is from the private collection of one of the authors (M.N.F.), but the single crystal used our study of gallobeudantite is in the Canadian Museum of Nature, Ottawa; as well, a polished section of the sulfide-rich matrix of the specimen, and sections containing the analyzed grains described here, are in the Systematic Reference Series of the National Mineral Collection of Canada, housed at the Geological Survey of Canada, Ottawa. The original specimen was labeled “fleischerite” and is believed to have been collected in about 1960, when fleischerite was first described; the level of the mine from which the specimen was extracted is not known. Tsumeb is a world-famous mineral locality partly because of the unusual geochemistry of its primary ores, and partly because supergene alteration has led to the development of an extensive suite of secondary minerals, many of which are of display quality. Beudantite, and now gallobeudantite, are among the minerals in the secondary suite.

GALLOBEUDANTITE

Gallobeudantite occurs in vugs in a single, blackish specimen of massive copper ore, approximately $3 \times 5 \times 1.5$ cm. The vugs are megascopically inconspicuous, and the crystals within the vugs are not noticeable unless examined with a binocular microscope. A polished section of one end of the specimen showed that the host material consists

TABLE 1. ELECTRON-MICROPROBE COMPOSITIONS OF MATRIX SULFIDES

	renierite			gallite			germanite-like		
	Gr. 1	Gr. 2	Gr. 3	Gr. 1	Gr. 2	Gr. 3	Gr. 1	Gr. 2	Gr. 3
Cu, wt. %	42.5	42.4	42.3	32.7	32.6	32.1	62.4	61.9	63.8
Zn	2.0	2.0	2.1	0.7	1.7	2.3	0.5	0.4	0.4
Fe	13.3	13.5	13.2	1.4	1.7	1.7	2.0	1.7	1.6
Ga	0.4	0.5	0.5	32.7	31.2	31.0	0.4	0.4	0.3
Ge	7.5	7.6	7.9	0.4	0.6	0.7	6.4	6.3	6.1
As	1.8	1.9	1.7	0.0	0.0	0.0	1.6	1.6	1.4
S	<u>32.6</u>	<u>32.4</u>	<u>32.8</u>	<u>33.1</u>	<u>32.9</u>	<u>32.9</u>	<u>27.4</u>	<u>27.0</u>	<u>26.3</u>
S sum	100.1	100.3	100.5	101.0	100.7	100.7	100.7	99.3	99.9
	formula, 33 atoms			formula, 4 atoms			formula, 20 atoms		
Cu	10.57	10.55	10.49	Cu 1.00	1.00	0.98	Cu 6.89	6.94	7.15
Zn	<u>0.49</u>	<u>0.49</u>	<u>0.50</u>				Zn <u>0.06</u>	<u>0.04</u>	<u>0.04</u>
	11.06	11.04	10.99	Ga 0.91	0.87	0.87	6.95	6.98	7.19
				Fe 0.05	0.06	0.06			
Fe	3.76	3.83	3.72	Zn 0.02	0.05	0.07	Ge 0.62	0.62	0.60
Ga	<u>0.02</u>	<u>0.11</u>	<u>0.11</u>	Ge <u>0.01</u>	<u>0.02</u>	<u>0.02</u>	Fe 0.25	0.21	0.21
	3.85	3.94	3.83	0.99	1.00	1.02	Ga 0.04	0.04	0.03
							As <u>0.15</u>	<u>0.15</u>	<u>0.14</u>
Ge	1.63	1.66	1.72	S 2.01	2.00	2.00	1.06	1.02	0.98
As	<u>0.38</u>	<u>0.40</u>	<u>0.36</u>						
	2.01	2.06	2.08				S 12.00	12.00	11.68
S	16.07	15.97	16.11						

Analyses at 20 kV, 20 nA, 20-second count rate, Tracor Northern PRZ correction program. Standards: chalcopyrite (Cu,Fe,S), synthetic FeAs₂ (As), Ge metal (Ge), synthetic Tm₃Ga₂O₁₂ (Ga), sphalerite (Zn).

mainly of aligned inclusions of renierite, up to 1×3 mm, in a granular matrix consisting largely of a mineral that gives a germanite-like X-ray powder pattern, but with a composition much too Cu-rich to be germanite (Table 1); the latter is under further study. The renierite (Table 1) contains irregular inclusions of gallite (Table 1) up to 75 μm across, and one end of the section is texturally complex and contains inclusions of Sb-free gallian (0.3 wt.% Ga) tennantite. A thin rim of chalcocite emphasizes the granular texture of the germanite-like phase, and all minerals are cut by irregular, hairline veinlets of chalcocite.

Disseminated on the surface of the specimen are local, minute patches of hematite and goethite, sparse crystals of stoltzite, and dots of spongy mercurian silver. One end of the specimen has a thin, discontinuous veinlet, about 1 mm long, of otjismeite, PbGe_4O_9 .

Physical and optical properties

Gallobeudantite occurs in the vugs as zones within crystals that show an extensive range of mutual solid-solution involving As, P, and S. The crystals are sparsely disseminated rhombohedra up to 200 μm along an edge. Some of the rhombohedra show a minor modification by {001}. Single, compositionally zoned crystals do occur, but most are multiple grains, too sparse to be described as aggregates. Most crystals are <100 μm in size, and have a Ca–Ga–AsO₄ beudantite-type analogue as the outermost zone. Gallobeudantite is pale yellow, to slightly greenish, to cream-colored, and is transparent, with a vitreous luster, white to pale yellow streak, and a Mohs hardness of 4. The mineral is brittle, giving an even to conchoidal fracture; the

evenness may be an indication of the {001} cleavage that is present in other members of the beudantite group. Density could not be measured because of the small grain-size; for $Z = 3$, D_{calc} is 4.87 g/cm^3 for the idealized formula and $\text{AsO}_4:\text{SO}_4 = 1:1$. Gallobeudantite is nonfluorescent, and in immersion oil is nonpleochroic, uniaxial negative, ω 1.763(5), ϵ 1.750(5) at 589 nm.

Composition

Electron-microprobe compositions for gallobeudantite were obtained with an JEOL 733 instrument operated at 15 kV and with a beam current of 20 nA, using 10-second counting times, the Tracor Northern PROZA correction program, and the following standards: apatite (P) from Durango, Mexico, Ge metal (Ge), and synthetic GaAs (Ga), ZnFe_2O_4 (Zn,Fe), PbSO_4 (Pb,S), Al_2O_3 (Al), InAs (As), and CaTiSiO_5 (Ca). As most of the analyzed zones were found to be slightly unstable under the electron beam, analyzed areas were restricted as much as possible to those with dimensions large enough to permit movement of the specimen during data acquisition. Gallobeudantite was among the least stable phases, and the PO_4 analogue was the most stable.

Figures 1 to 7, inclusive, illustrate typical zoned grains containing gallobeudantite, for which electron-microprobe compositions are given in Table 2. The average composition derived from six analyses in

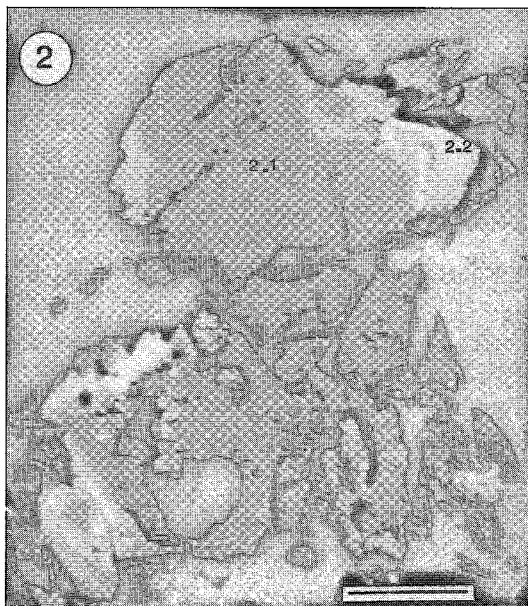


FIG. 2. BSE image of poorly polished grain consisting of Ga analogue of segnitite (area 2.2, Table 2) and gallian hidalgoite (2.1, Table 3). Bar scale represents 50 μm .

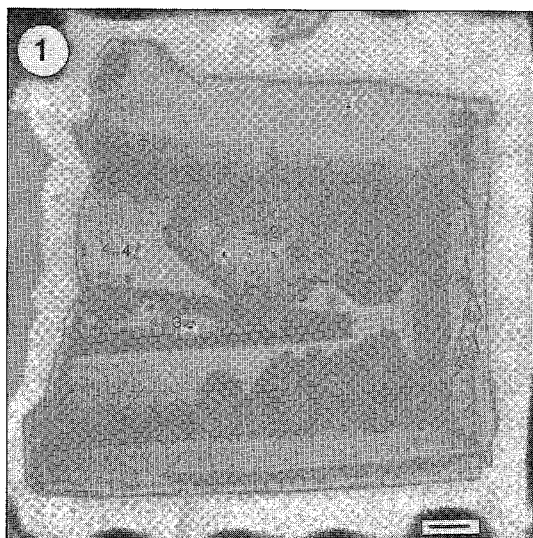


FIG. 1. Back-scattered-electron (BSE) image of zoned grain containing areas of gallobeudantite (analyses 4.2, 4.4, and 4.7 in Table 2). Zone 4.3 is a PO_4 analogue (Table 3). A narrow outermost zone, not visible in the photograph, consists of the Ga analogue of arsenocrandallite. Bar scale represents 10 μm .

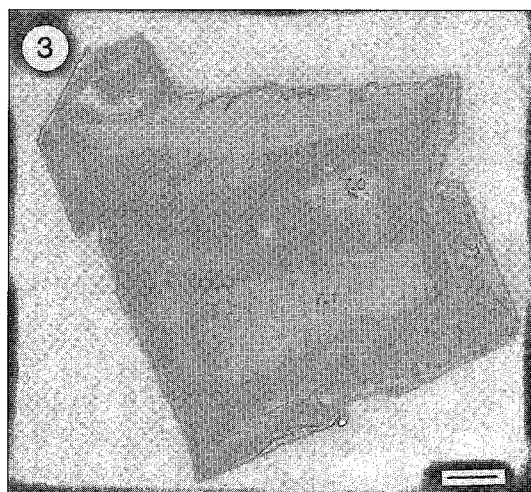


FIG. 3. BSE image of zoned grain consisting of gallobeudantite (7.1, Table 2), gallian beudantite (7.0, Table 3), and gallian hidalgoite (7.2, Table 3). Outermost zone (7.3) is the Ca analogue of gallobeudantite. Bar scale represents 20 μm .

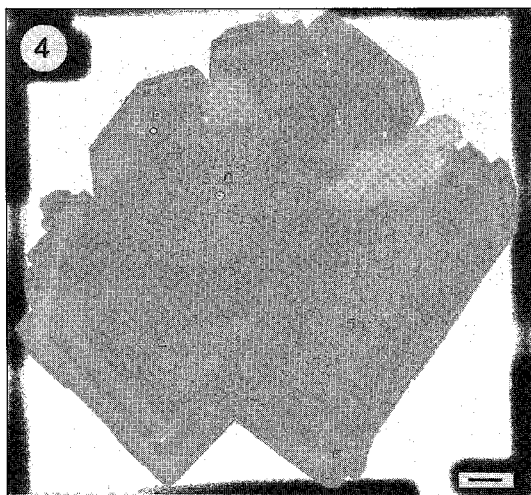


FIG. 4. BSE image of zoned grain consisting of gallobeudantite (5.4, Table 2; 5.0 and 5.2 are similar). Dark, outer zone (5.7) is gallian hidalgite. Bar scale represents 20 μm .

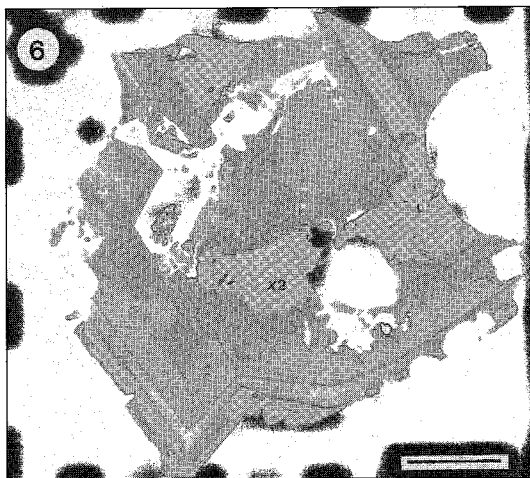


FIG. 6. BSE image of zoned grain in which dark core (X) consists of PO_4 analogue of gallobeudantite (PS3-A1 in Table 4), and light grey zone (X 2) is gallobeudantite. Bar scale represents 50 μm .

Table 2 is $\text{Pb}_{1.04}(\text{Ga}_{1.49}\text{Fe}_{0.82}^{3+}\text{Al}_{0.62}\text{Zn}_{0.10})_{\Sigma 3.03}[(\text{AsO}_4)_{1.14}(\text{SO}_4)_{0.86}]_{\Sigma 2.00}(\text{OH})_{5.94}$, which is the Ga analogue of beudantite, idealized as $\text{PbFe}_3^+[(\text{AsO}_4)(\text{SO}_4)]_2(\text{OH})_6$. As is evident from Table 2, Ga, Fe, and Al show considerable mutual substitution in the mineral, whereas that involving Zn and Ge is minor. The XO_4

position is characterized by a predominance of (AsO_4) , substantial substitution of (SO_4) for (AsO_4) , and negligible (PO_4) . The predominance of (AsO_4) in zone 6.1 (Table 2) is sufficiently large that the composition corresponds to the Ga analogue of segnitite, the latter ideally $\text{PbFe}_3^+\text{H}(\text{AsO}_4)_2(\text{OH})_6$. The compositions of

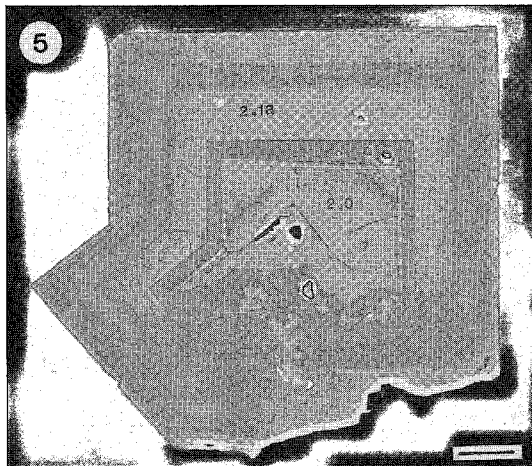


FIG. 5. BSE image of zoned grain consisting of core of gallian beudantite (2.0, Table 3) rimmed by PO_4 analogue of gallobeudantite (2.2, Table 4), which is in turn rimmed by gallobeudantite (2.1a, Table 2); area 2.3 is Al-rich (up to 10 wt.% Al_2O_3) gallobeudantite. Bar scale represents 20 μm .



FIG. 7. BSE image showing PO_4 analogue of gallobeudantite (PS3-D, Table 4) and a whiter zone of gallobeudantite. Bar scale represents 10 μm .

TABLE 2. ELECTRON-MICROPROBE COMPOSITIONS OF GALLOBEUDANTITE

	Fig. 1		Fig. 2		Fig. 3	Fig. 4	Fig. 5		cr3
	4.2	4.4	4.7	2.2*	7.1	5.4	2.1a	6.1	
PbO, wt%	32.1	30.8	32.2	29.7	30.4	30.3	30.4	29.6	30.8
CaO	0.0	0.0	0.0	0.0	0.0	0.0	0.0	0.0	0.0
ZnO	2.2	0.6	2.0	0.0	0.6	0.6	0.5	0.0	3.4
Ga ₂ O ₃	19.2	18.4	20.0	19.5	18.5	19.8	19.8	17.6	31.6
Fe ₂ O ₃	2.9	12.2	3.7	4.7	13.3	10.6	10.7	4.0	1.3
Al ₂ O ₃	8.9	2.3	8.1	5.5	1.5	3.0	3.0	7.6	0.9
As ₂ O ₃	16.0	18.6	16.6	25.0	18.1	18.7	20.2	23.9	9.2
SO ₃	10.5	9.7	10.7	5.0	9.0	9.0	8.2	5.7	13.7
P ₂ O ₅	0.2	0.0	0.5	0.2	0.0	0.0	0.0	0.0	0.9
GeO ₂	0.6	0.0	0.0	2.6	0.0	0.0	0.0	2.9	0.0
[H ₂ O] _{calc}	8.3	6.7	7.8	6.5	7.1	7.1	6.9	7.0	7.9
	100.9	99.3	101.6	98.7	98.5	99.1	99.7	98.3	99.7
<i>formula for 14 oxygens</i>									
Pb	1.00	1.03	1.00	1.11	1.03	1.00	1.17	0.98	0.98
Zn	0.19	0.06	0.17	—	0.07	0.06	0.04	—	0.29
Ga	1.43	1.47	1.48	1.59	1.49	1.56	1.53	1.39	2.40
Fe	0.25	1.14	0.32	0.45	1.26	0.98	0.97	0.37	0.12
Al	1.21	0.33	1.10	0.74	0.22	0.44	0.43	1.10	0.13
Ge	0.04	—	0.05	0.19	—	—	—	0.20	—
	3.12	3.00	3.12	2.97	3.04	3.04	2.97	3.06	2.94
As	0.96	1.21	1.00	1.66	1.19	1.20	1.28	1.55	0.57
S	0.91	0.91	0.93	0.48	0.85	0.83	0.75	0.53	1.22
P	0.02	—	—	0.02	—	—	—	—	0.21
	1.89	2.12	1.93	2.16	2.04	2.03	2.03	2.08	2.00
(OH)	6.41	5.55	6.12	5.57	5.86	5.77	5.90	5.69	5.72

*Composition corresponds to Ga analogue of segnitite.

TABLE 4. ELECTRON-MICROPROBE COMPOSITIONS OF Pb-Ga PHOSPHATE

	Fig. 1	Fig. 5	Fig. 6	Fig. 7	Avg.	
	4.3	2.2	PS3-A1	PS 3-6 PS3-D		
PbO, wt. %	31.7	33.1	32.5	32.3	33.2	32.56
CaO	0.0	0.0	0.0	0.0	0.0	—
ZnO	0.0	0.0	0.0	0.0	0.0	—
GeO ₂	0.0	0.0	0.0	0.0	0.0	—
Ga ₂ O ₃	24.5	26.3	26.9	26.3	27.4	26.28
Fe ₂ O ₃	10.7	9.2	7.6	6.4	7.0	8.18
Al ₂ O ₃	1.7	2.6	3.0	3.2	2.6	2.62
As ₂ O ₃	1.1	0.0	0.0	0.0	0.8	0.38
SO ₃	5.5	6.0	6.5	6.5	5.5	6.00
P ₂ O ₅	14.0	15.8	15.2	14.2	15.4	14.96
[H ₂ O] _{calc}	89.2	93.0	91.7	88.9	91.9	90.98
						7.36
						98.34
<i>formula for 14O</i>						
Pb	1.04	1.03	1.02	1.04	1.07	1.04
Ga	1.91	1.96	2.02	2.03	2.10	2.00
Fe	0.98	0.80	0.67	0.62	0.63	0.73
Al	0.24	0.36	0.42	0.45	0.37	0.37
	3.13	3.12	3.11	3.10	3.10	3.10
P	1.44	1.55	1.52	1.44	1.55	1.51
S	0.50	0.51	0.57	0.58	0.49	0.54
As	0.07	—	—	—	0.05	0.02
	2.01	2.06	2.09	2.02	2.09	2.07
OH	5.95	5.74	5.64	5.89	6.20	5.74

various zones in the gallobaudantite-bearing grains (Tables 2, 3, 4), and the implications for nomenclature, are discussed in later sections.

TABLE 3. ELECTRON-MICROPROBE COMPOSITIONS OF GALLIAN HIDALGOITE AND BEUDANTITE

	Hidalgoite			Beudantite	
	Fig. 3	Fig. 2	Fig. 4	Fig. 3	Fig. 5
PbO, wt. %	7.2	2.1	5.7	7.0	2.0
CaO	0.0	0.0	0.0	0.0	0.0
ZnO	0.9	0.0	0.5	0.0	0.2
Ga ₂ O ₃	15.2	12.6	18.3	12.6	11.2
Fe ₂ O ₃	3.6	5.9	2.6	19.7	22.2
Al ₂ O ₃	11.1	11.3	10.8	1.5	0.2
As ₂ O ₃	18.9	17.5	17.5	20.6	20.2
SO ₃	9.0	11.0	9.7	6.5	8.0
P ₂ O ₅	0.2	0.0	0.5	0.9	0.2
GeO ₂	0.3	0.0	0.0	0.0	0.6
	92.7	91.2	92.6	93.4	92.4
Pb	1.05	1.02	1.02	1.06	0.99
Zn	0.07	—	0.04	—	0.02
Ga	1.13	0.94	1.35	1.01	0.89
Fe	0.31	0.51	0.22	1.85	2.07
Al	1.53	1.55	1.46	0.22	0.03
Ge	0.02	—	—	—	0.04
	3.06	3.00	3.07	3.08	3.05
As	1.15	1.06	1.05	1.34	1.32
S	0.79	0.95	0.84	0.61	0.75
P	0.02	—	0.04	0.10	0.02
	1.96	2.01	1.93	2.05	2.09
(OH) _{calc}	6.17	5.95	6.24	5.84	5.65

X-ray data

Debye-Scherrer X-ray patterns obtained with 114.6-mm cameras and CoK α radiation indicate that the compositional variations in the zoned crystals do not have an extreme effect on the cell dimensions. Although the X-ray powder patterns of aggregates of the zoned crystals are not sharp relative to, e.g., the powder pattern of quartz, neither are they unusually broad or diffuse, and there are no signs of the multiple lines that would appear if solid solution radically shifted the cell dimensions. None of the diffraction patterns was observed to have an 11 Å diffraction line, the presence of which would indicate a doubling of the *c* axis to ~34 Å, as occurs in some members of the beudantite group and in the alunite - jarosite family, with plumbojarosite perhaps the best known example.

The crystal structure of gallobaudantite was determined from a fragment extracted from the area marked 4.7 in Figure 1. The material extricated from area 4.7, which also included a small amount of powder, gave a Gandolfi pattern that is spotty but otherwise matches well the pattern of a bulk sample as listed in Table 5. Gallobaudantite is rhombohedral, space group *R3m*. The crystal-structure determination gave *a* 7.225(4), *c* 17.03(2) Å, *V* 770(1) Å³. An energy-dispersion analysis of this single-crystal fragment confirmed the absence of P.

TABLE 5. REPRESENTATIVE X-RAY POWDER DATA FOR GALLOBEUDANTITE

I_{est}	d_{meas}	d_{calc}	hkl
90	5.85	5.85	101
15	5.00	5.03	012
40	3.59	3.59	110
5	3.52	3.52	104
100	3.038	3.038	113
25	2.920	2.923	202*
30	2.851	2.846	006*
30	2.513	2.514	024*
10	2.329	2.330	211*
1	2.299	2.300	205
40	2.271	2.271	107*
15	2.231	2.231	116*
5	2.063	2.060	214
30	1.948	1.949	303*
30	1.797	1.796	220*
5	1.759	1.760	208*
1	1.715	1.717	131
5	1.693	1.693	217*
10	1.678	1.678	119*
1	1.646	1.647	1.0.10
10	1.519	1.519	226*
15	1.497	1.497	0.2.10*
5	1.409	1.409	137
		1.408	232
5	1.400	1.400	039*
2	1.384		
8	1.320		
3	1.285		

*114.6-mm Debye-Scherrer camera, CoK_{α} X-radiation. Lines with an asterisk were used for the unit-cell refinement; indexed with a 7.184, c 17.077 Å.

Crystal structure

The fragment of gallobseudantite used for the collection of X-ray-diffraction intensity data is designated as CMNMI 81518. Single-crystal precession photographs gave the space-group choices $R32$ (155), $R3m$ (160), and $R\bar{3}m$ (166) on the basis of systematic absences of reflections. Intensity data were collected on a fully automated Nicolet $R3m$ four-circle diffractometer. A set of 22 reflections was used to orient the crystal and to refine the cell dimensions. Three asymmetric sets of intensity data were collected up to $2\theta = 55^\circ$ using a $\theta:2\theta$ scan-mode and variable scan speeds of 3 to $29^\circ/\text{minute}$. Data pertinent to the collection of the intensity data are given in Table 6. For the absorption correction, four intense diffraction-maxima in the range 13 to $50^\circ 2\theta$ were chosen for ψ diffraction-vector scans after the method of North *et al.* (1968). Structure determination and structure refinement were done using the SHELXTL (Sheldrick 1990) package of computer programs. The crystal's irregular shape, precluding a good absorption-correction, became the limiting factor in the structure refinement. This problem in the data reduction is evident from a merging R of 13.1% for the three asymmetric units of reflection data.

TABLE 6. GALLOBEUDANTITE: STRUCTURE-DETERMINATION DATA

Ideal formula:	$N PbGa_3[(AsO_4)_2(SO_4)]_2(OH)_6$	$a = 7.225(4) \text{ \AA}$
Space group:	$R\bar{3}m$ (160)	$c = 17.03(2) \text{ \AA}$
Crystal size:	$0.12 \times 0.12 \times 0.06 \text{ mm}$	$V = 770(1) \text{ \AA}^3$
		$Z = 4$
Radiation:	Mo/graphite monochromator	Total refl. 1290
Operating conditions:	50 kV/40 mA	F unique 496
μ :	28 mm^{-1}	$R(\text{int})$ 13.1%
Min. transmission:	0.143	$F_o > 6\sigma(F)$ 416
Max. transmission:	0.803	
		Final $R = 7.8\%$
		Final $wR = 6.7\%$

Normalized structure-factor statistics, $|E^2 - 1| = 0.793$, indicate an acentric space-group. The E -map coordinates were assigned to appropriate scattering curves, Pb, Ga, As, S and six O atoms in $R\bar{3}m$. This structure model refined to $R = 8.0\%$. The equivalent model in $R3$ refined to $R = 10.0\%$, and in $R\bar{3}m$, to $R = 9.1\%$. In the final least-squares refinement, the sites of all cations were refined with anisotropic displacement-factors. The addition of an isotropic extinction-correction did not improve the refinement. In the final ΔF -synthesis, residual electron densities remained, but none of these could be satisfactorily assigned to H atoms. The final positional and displacement parameters for the gallobseudantite structure are given in Table 7, and selected bond-lengths and angles, in Table 8. Observed and calculated structure-factors have been submitted to the Depository of Unpublished Data, CISTI, National Research Council of Canada, Ottawa, Canada K1A 0S2.

Gallobseudantite is isostructural with corkite, $PbFe_3[(SO_4)_2(PO_4)]_2(OH)_6$, (Giuseppetti & Tadini 1987), with Ga replacing Fe and As replacing P within the crystal structure. The Pb site refines off the origin,

TABLE 7. GALLOBEUDANTITE: ATOMIC COORDINATES AND ISOTROPIC DISPLACEMENT FACTORS ($\text{\AA} \times 10^4$)

ATOM	x	y	z	U_{eq}
Pb	0.020(4)	-0.014(6)	0	402(53)
Ga	0.9978(7)	0.4989(4)	0.4991(3)	154(9)
As	0	0	0.6825(3)	84(10)
S	0	0	0.3011(8)	206(23)
O1	0	0	0.579(1)	200
O2	0	0	0.394(1)	200
O3	0.752(3)	0.876(1)	0.7196(9)	159(35)
O4	0.216(2)	0.784(2)	0.9418(9)	288(44)
OH1	0.455(2)	0.909(3)	0.803(1)	260(42)
OH2	0.873(1)	0.746(2)	0.866(1)	36(27)

TABLE 8. GALLOBEUDANTITE: SELECTED BOND LENGTHS (Å) AND BOND ANGLES(°)

Pb-O ICOSAHEDRON			
Pb-O3	2.66(3)	Pb-OH1	2.82(3)
Pb-O3	2.97(5)	Pb-OH1	2.84(3)
Pb-O3	2.69(4)	Pb-OH1	2.66(3)
Pb-O4	2.68(4)	Pb-OH2	2.73(2)
Pb-O4	2.96(4)	Pb-OH2	2.71(2)
Pb-O4	2.99(3)	Pb-OH2	2.90(3)
⟨Pb-O⟩	⟨2.825⟩	⟨Pb-OH⟩	⟨2.777⟩
Ga-O OCTAHEDRON			
Ga-O3	1.998(17)	O3-O4	178.1(7)
Ga-O4	1.956(16)	O3-OH1	86.1(7) x 2
Ga-OH1	1.927(8) x 2	O3-OH2	95.7(6) x 2
Ga-OH2	1.982(7) x 2	O4-OH1	92.5(7) x 2
		O4-OH2	85.7(6) x 2
⟨Ga-O⟩	⟨1.962⟩	OH1-OH1	86.1(6)
		OH1-OH2	177.9(6) x 2
		OH1-OH2	93.0(6) x 2
		OH2-OH2	87.9(5)
As-O TETRAHEDRON			
As-O1	1.76(2)	O1-O3	112.2(6) x 3
As-O3	1.68(2) x 3	O3-O3	106.6(6) x 3
⟨As-O⟩	⟨1.70⟩	⟨O-O⟩	⟨109.4⟩
S-O TETRAHEDRON			
S-O2	1.58(3)	O2-O4	106.7(7) x 3
S-O4	1.54(1) x 3	O4-O4	112.2(7) x 3
⟨S-O⟩	⟨1.55⟩	⟨O-O⟩	⟨109.4⟩

as was found for the centric structure of beudantite (Szymański 1988). This shift within the polyhedron is a result of the stereochemically inactive lone-pair electrons associated with Pb, an effect that has been noted in the structure of several minerals (Grice *et al.* 1991). As in corkite and beudantite, the Pb-O polyhedron is an icosahedron with the six Pb-O bond lengths being longer than the six Pb-OH bond lengths: gallobeudantite 2.82 Å *versus* 2.78 Å, corkite 2.92 Å *versus* 2.73 Å (Giuseppetti & Tadani 1987), and beudantite 2.87 Å *versus* 2.80 Å (Szymański 1988). The Ga site-occupancy refines to an atomic scattering power of 24.8 electrons, which compares well with the microprobe results of 25.1 electrons for the combined elements Ga, Al, Fe, Zn, and Ge in the analysis of area 4.7 in Figure 1 (Table 2). The Ga polyhedron is a slightly distorted octahedron (Table 8). The Ga polyhedra form (001) sheets of corner-sharing polyhedra (Fig. 8). The two tetrahedra sites [AsO₄] and [SO₄] are aligned along [001] (Fig. 9). The sites are well ordered, with site-occupancy refinements of 31.9(7) electrons (As site) and 16.5(7) electrons (S site). The refinements are both within 2σ of the ideal scattering power of As and S, respectively. Similarly, ordering of the sites is demonstrated by the average bond-lengths, 1.70 Å for As-O and 1.55 Å for S-O, which are in keeping with other arsenates and sulfates. It is the ordering of these two tetrahedron sites that lowers the symmetry from *R*3̄*m* to *R*3*m*.

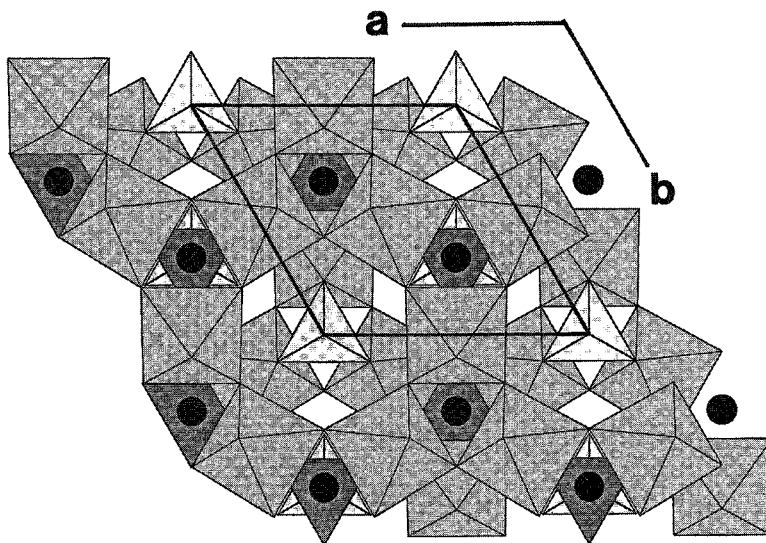


FIG. 8. A projection of the gallobeudantite structure along [001] showing corner-sharing layers of Ga octahedra alternating with layers of (AsO₄) tetrahedra (dark shading), (SO₄) tetrahedra (light shading), and Pb atoms (filled circles).

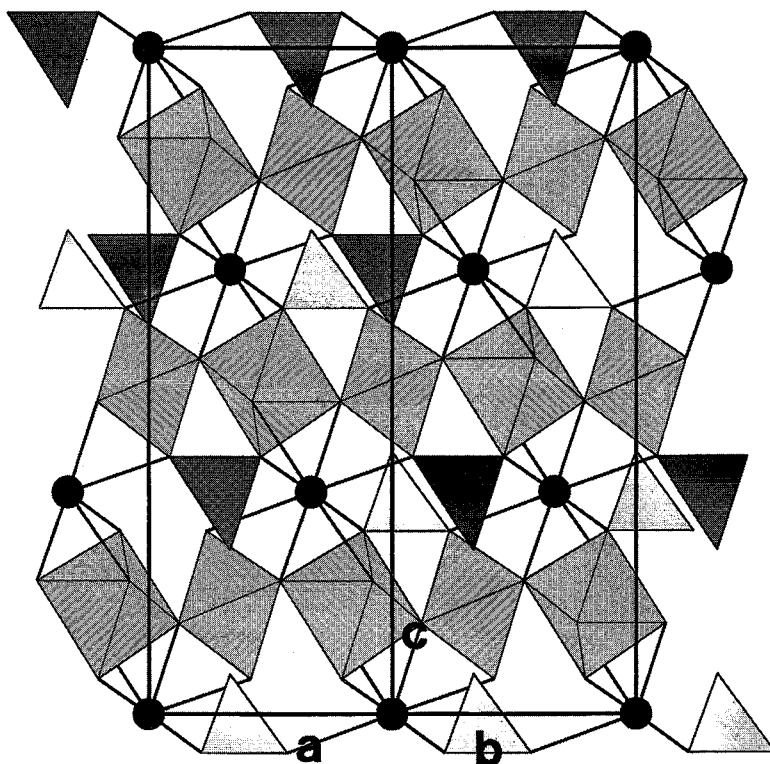


FIG. 9. A projection of the gallobeudantite structure along $[110]$, showing layers of corner-sharing Ga octahedra. The (AsO_4) tetrahedra (dark shading), (SO_4) tetrahedra (light shading), and Pb atoms (filled circle) are aligned along $[001]$.

NOMENCLATURE

Beudantite has the ideal formula $\text{PbFe}(\text{AsO}_4)(\text{SO}_4)_2(\text{OH})_6$, and the structure is rhombohedral, space group $R\bar{3}m$ (Szymański 1988, Giuseppetti & Tadini 1989). Although ordering of As and S lowers the symmetry of gallobeudantite to $R3m$, the effects of order can be more pronounced, and may lead to a doubling of the c axis or to changes in symmetry (e.g., Cowgill *et al.* 1963, Radoslovich 1982, Jambor & Dutrizac 1983). To accommodate changes in symmetry and the compositional variations, various subdivisions of the alunite – jarosite family (which includes beudantite and corkite) have been proposed (e.g., Scott 1987, Novák *et al.* 1994). The system of nomenclature applicable to this family is currently under review (Jambor *et al.* 1995). Although the IMA-approved nomenclature is not consistent in all cases (Jambor *et al.* 1996), in this paper we rigidly follow Scott's (1987) IMA-approved system for composition boundaries, despite its limitations (Birch *et al.* 1992, Pring *et al.* 1995). Thus, the simple Pb-dominant

ternary system as shown in Figure 10 ignores symmetry and cell-dimension variations such as doubling of the c axis. The boundary between Fe^{3+} -dominant species (Fig. 10) and Al-dominant species (Fig. 12) is set at 1:1; similarly, Ga-dominant species (Fig. 11) would have $\text{Ga} > \text{Fe}^{3+}$ or $\text{Ga} > \text{Al}$, regardless of the sum of $\text{Fe}^{3+} + \text{Al}$.

Solid solution

The A position in the formula of the alunite – jarosite family may be filled by monovalent ions such as K, Na, and (H_3O) , or by divalent ions such as Pb, Ba, Sr, and Ca. Figure 10 shows the nomenclature for the (XO_4) ternary system in which Pb is dominant in the A position and Fe^{3+} is dominant in B. The two points plotted correspond to gallian beudantite (up to 12.6 wt.% Ga_2O_3 ; Table 3). The analogous diagram, but with $\text{Ga} > \text{Fe}^{3+}$, is shown in Figure 11. Compositions of gallobeudantite fall mainly along or near the $\text{SO}_4 - \text{AsO}_4$ join, extending along its lower half and into the field of the Ga analogue of segnitite

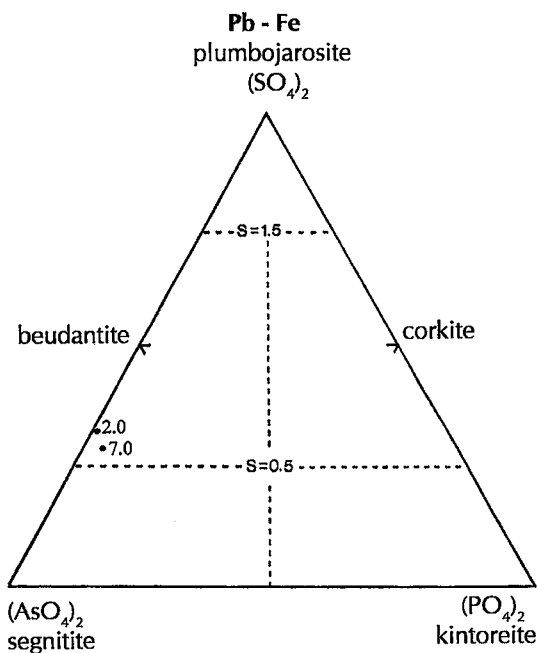


FIG. 10. Nomenclature for the Fe³⁺-dominant portion of the Pb-XO₄ members of the alunite - jarosite family. Plotted points 2.0 and 7.0 are compositions of Ga-rich beudantite (Table 3).

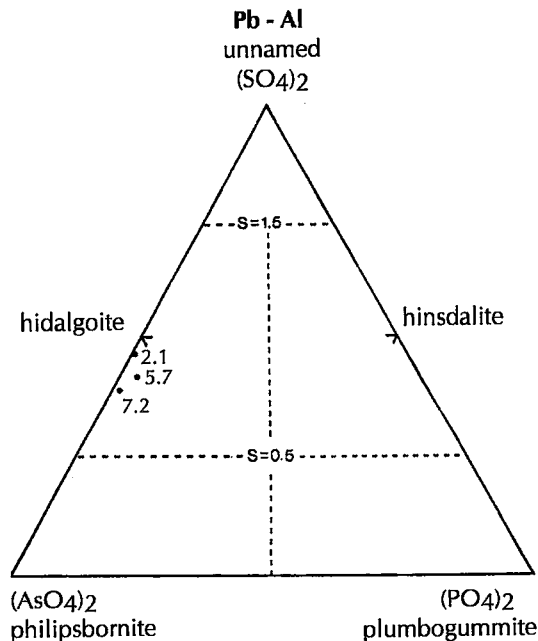


FIG. 12. Nomenclature for the Al-dominant portion of the Pb-XO₄ members of the alunite - jarosite family. Plotted points correspond to compositions in Table 3, but with XO₄ normalized to 2.00.

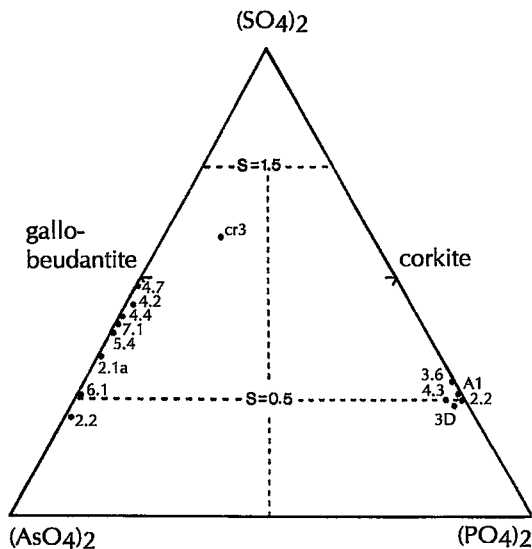


FIG. 11. Compositions of members of the Pb-XO₄ system, as in Figure 8, but with Ga > Fe³⁺. Plotted points correspond to compositions in Tables 2 and 4, but with XO₄ normalized to 2.00. Gallobeudantite is the only named mineral in the system.

(Fig. 11, Table 2). In the opposite direction, the most SO₄-rich sample (cr3) is compositionally and megascopically distinct, occurring on the specimen as a cream-colored isolated patch about a millimeter in diameter. The patch is a granular aggregate in which the grains are 5–10 μm across, are anhedral, brittle, and lack cleavage. In transmitted light, the grains are colorless and uniaxial positive, with ω 1.786(5) and ϵ 1.790(5) at 589 nm. Thus, the higher indices of refraction and change in optic sign distinguish this phase from gallobeudantite, less rich in SO₄ and PO₄, but no differences were observed in the 114.6-mm X-ray powder-diffraction patterns of the two types.

Solid solution involving As-for-P substitution in the zoned crystals is minimal in areas that can be analyzed quantitatively with confidence. Thus, Figure 11 shows clustering of compositions either along the As-rich join or the P-rich join, with no As - P intermediate values. The P-rich compositions correspond to the unnamed Ga analogue of corkite and the unnamed Ga analogue of kintoreite.

Substitutions among Ga, Fe, and Al are extensive, and any of these may predominate in B. Thus, compositions extend from gallian beudantite (Fe³⁺ > Ga > Al), to gallobeudantite (Ga > Fe³⁺ > Al,

TABLE 9. ELECTRON-MICROPROBE COMPOSITIONS OF Ca-Ga ARSENATE

	Gr	Gr	Gr	Gr	Gr	Avg.	Formula, 14 O	
	4.1	6	2	3.1	1.2			
PbO, wt. %	2.4	1.5	2.8	2.6	2.8	2.42	Pb 0.07	1.04
CaO	8.3	9.0	8.5	7.7	8.5	8.40	Ca 0.97	
GeO ₂	12.4	11.7	12.0	12.7	12.0	12.16	Ge 0.75	2.97
Ga ₂ O ₃	23.5	22.4	23.8	25.0	23.8	23.70	Ga 1.64	
Fe ₂ O ₃	2.4	5.0	3.1	2.9	3.1	3.30	Fe 0.27	
Al ₂ O ₃	3.0	2.5	2.6	1.5	2.6	2.44	Al 0.31	
As ₂ O ₃	38.8	38.0	37.1	39.0	37.1	38.00	As 2.14	2.20
SO ₃	1.0	0.7	0.7	0.7	0.7	0.76	S 0.06	
P ₂ O ₅	0.0	0.0	0.0	0.2	0.0	0.04	P 0.00	
	91.8	90.8	90.6	92.3	90.6	91.22	(OH) _{sub}	5.18

and Ga > Al > Fe³⁺), to gallian hidalgite (Al > Ga > Fe³⁺; Fig. 12).

In gallobaudantite and its associated minerals, the A position is occupied solely by Pb (Tables 2, 3, 4); however, some of the crystals have a narrow outermost zone, invariably less than 10 μm wide, in which Ca predominates in the A position. This mineral is unstable under the electron beam, and the narrowness of the zones and the instability make analyses difficult. Nevertheless, the results (Table 9) show a consistent

predominance in Ca and As, with Ga the main element in the B position. Contents of Ge are up to 12.7 wt.% GeO₂ (Table 9); although some substitution for As would be expected on the basis of their similar ionic radii (Bernstein 1985), it is evident that Ge⁴⁺ in the boudantite-type minerals substitutes for the trivalent ions in the B position. This Ca-rich mineral is in essence a Ca-Ga arsenate that, if Ge were absent, would correspond to the Ca analogue of the unnamed Ga analogue of segnitite (Figs. 10, 11) or, more simply, to the Ga analogue of arsenocrandallite (Fig. 13). The ideal end-member formula of the latter can be written as CaGa₃H(AsO₄)₂(OH)₆. Substitution of Ge⁴⁺ for Ga³⁺ is substantial, but is constrained by charge-balance limits so that the maximum Ge content probably corresponds to Ca(Ga,Al,Fe)₂Ge(AsO₄)₂(OH)₆. Table 9 shows that the composition of the Tsumeb mineral reaches 75% of the probable allowable limit of Ge substitution.

ACKNOWLEDGEMENTS

We thank CANMET personnel P. Carrière for assistance with the X-ray powder studies, and J.M. Greer for preparation of the polished sections. Dr. F.C. Hawthorne of the Department of Geological Sciences, University of Manitoba, kindly arranged for the use of the four-circle diffractometer. The critical reviews and editorial comments by A.C. Roberts, W.D. Birch, A. Pring, and R.F. Martin are much appreciated.

REFERENCES

- BERNSTEIN, L.R. (1985): Germanium geochemistry and mineralogy. *Geochim. Cosmochim. Acta* **49**, 2409-2422.
- (1986): Geology and mineralogy of the Apex germanium-gallium mine, Washington County, Utah. *U.S. Geol. Surv., Bull.* **1577**.
- BIRCH, W.D., PRING, A. & GATEHOUSE, B.M. (1992): Segnitite, PbFe₃H(AsO₄)₂(OH)₆, a new mineral in the lusungite group from Broken Hill, New South Wales, Australia. *Am. Mineral.* **77**, 656-659.
- COWGILL, V.M., HUTCHINSON, G.E. & JOENSUU, O. (1963): An apparently triclinic dimorph of crandallite from a tropical swamp sediment in El Petén, Guatemala. *Am. Mineral.* **48**, 1144-1153.
- DUTRIZAC, J.E. (1984): The behaviour of impurities during jarosite formation. In *Hydrometallurgical Process Fundamentals* (R.G. Bautista, ed.). Plenum Publ. Co., New York, N.Y. (125-169).
- , JAMBOR, J.L. & CHEN T.T. (1986): Host minerals for the gallium-germanium ores of the Apex mine, Utah. *Econ. Geol.* **81**, 946-950.

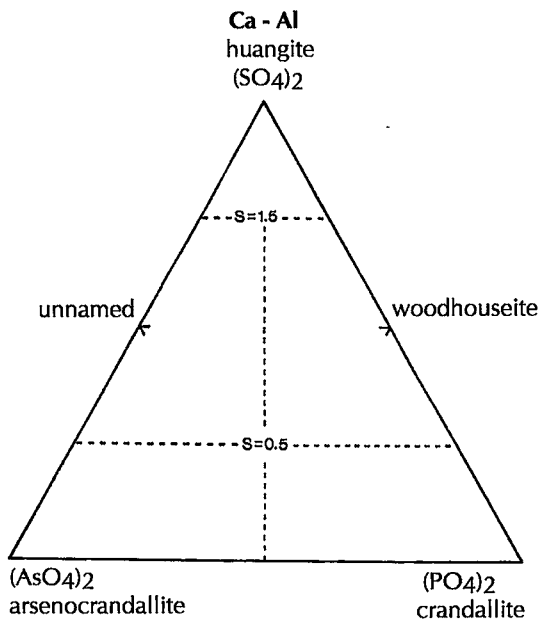


FIG. 13. Nomenclature for the Al-dominant portion of the Ca-XO₄ members of the alunite - jarosite family. The equivalent Fe³⁺ analogues are not known; compositions in Table 9 correspond to the Ga analogue of arsenocrandallite.

- GIUSEPPETTI, G. & TADINI, C. (1987): Corkite, $\text{PbFe}_3(\text{SO}_4)(\text{PO}_4)(\text{OH})_6$, its crystal structure and ordered arrangement of the tetrahedral cations. *Neues Jahrb. Mineral. Monatsh.*, 71-81.
- _____ & _____ (1989): Beudantite: $\text{PbFe}_3(\text{SO}_4)(\text{AsO}_4)(\text{OH})_6$, its crystal structure, tetrahedral site disordering and scattered Pb distribution. *Neues Jahrb. Mineral. Monatsh.*, 27-33.
- GRICE, J.D., NICKEL, E.H. & GAULT, R.A. (1991): Ashburtonite, a new bicarbonate-silicate mineral from Ashburton Downs, Western Australia: description and structure determination. *Am. Mineral.* **76**, 1701-1707.
- HOPKINS, J.L. (1985): Apex mine goes into production. *CIM Bull.* **78**(879), 86-87.
- JAMBOR, J.L. & DUTRIZAC, J.E. (1983): Beaverite – plumbojarosite solid solutions. *Can. Mineral.* **21**, 101-113.
- _____, KOVALENKER, V.A. & ROBERTS, A.C. (1995): New mineral names. *Am. Mineral.* **80**, 630-635.
- _____, PERTSEV, N.N. & ROBERTS, A.C. (1996): New mineral names. *Am. Mineral.* **81**, 249-254.
- NORTH, A.C.T., PHILLIPS, D.C. & MATHEWS, F.S. (1968): A semi-empirical method of absorption correction. *Acta Crystallogr.* **A24**, 351-359.
- NOVÁK, F., JIŘI, J. & PRACHAŘ, I. (1994): Classification and nomenclature of alunite – jarosite and related mineral groups. *Věstník Českého geol. ústavu* **69**, 51-57.
- PRING, A., BIRCH, W.D., DAWE, J., TAYLOR, M., DELIENS, M. & WALENTA, K. (1995): Kintoreite, $\text{PbFe}_3(\text{PO}_4)_2(\text{OH},\text{H}_2\text{O})_6$, a new mineral of the jarosite – alunite family, and lusungite discredited. *Mineral. Mag.* **59**, 143-148.
- RADOSLOVICH, E.W. (1982): Refinement of gorceixite structure in *Cm*. *Neues Jahrb. Mineral. Monatsh.*, 446-464.
- SCOTT, K.M. (1987): Solid solution in, and classification of, gossan-derived members of the alunite – jarosite family, northwest Queensland, Australia. *Am. Mineral.* **72**, 178-187.
- SHELDRICK, G.M. (1990): *SHELXTL, a Crystallographic Computing Package* (revision 4.1). Siemens Analytical Instruments, Inc., Madison, Wisconsin.
- SZYMAŃSKI, J.T. (1988): The crystal structure of beudantite, $\text{Pb}(\text{Fe},\text{Al})_3[(\text{As},\text{S})\text{O}_4]_2(\text{OH})_6$. *Can. Mineral.* **26**, 923-932.

Received November 21, 1995, revised manuscript accepted August 20, 1996.